

# Optical Coherence Tomography Angiography in Diabetic Retinopathy: A Prospective Pilot Study



AKIHIRO ISHIBAZAWA, TAIJI NAGAOKA, ATSUSHI TAKAHASHI, TSUNEAKI OMAE, TOMOFUMI TANI, KENJI SOGAWA, HARUMASA YOKOTA, AND AKITOSHI YOSHIDA

- **PURPOSE:** To evaluate how optical coherence tomography (OCT) angiography depicts clinical fundus findings in patients with diabetic retinopathy (DR).
- **DESIGN:** Prospective study evaluating imaging technology.
- **METHODS:** Forty-seven eyes of 25 patients with DR were scanned using a high-speed 840-nm-wavelength spectral-domain optical coherence tomography instrument (RTVue XR Avanti; Optovue, Inc, Fremont, California, USA). Blood flow was detected using the split-spectrum amplitude-decorrelation angiography algorithm. Fluorescein angiography (FA) images were also obtained in all eyes and the ability to visualize microaneurysms, retinal nonperfused areas, and neovascularization was compared with that of the en face OCT angiograms.
- **RESULTS:** In 42 eyes, microaneurysms detected by FA near the macula appeared as focally dilated saccular or fusiform capillaries on OCT angiograms of the superficial and/or deep capillary plexus. Retinal nonperfused areas visualized by FA appeared as lesions with no or sparse capillaries on OCT angiograms. Area measurement of retinal nonperfusion near the macula in 7 eyes revealed a difference between the extent of nonperfused areas in superficial and deep plexuses. In 4 eyes, the vascular structures of neovascularization at the optic disc were clearly visualized on OCT angiograms. Decreases and re-increases of flow in new vessels were quantified in an eye treated with anti-vascular endothelial growth factor.
- **CONCLUSIONS:** OCT angiography can clearly visualize microaneurysms and retinal nonperfused areas and enables closer observation of each layer of the retinal capillaries. Quantitative information on new vessels can also be obtained. OCT angiography may be clinically useful to evaluate the microvascular status and therapeutic effect of treatments for DR. (Am J Ophthalmol 2015;160(1):35–44. © 2015 by Elsevier Inc. All rights reserved.)

**D**IABETIC RETINOPATHY (DR) IS THE LEADING cause of blindness in the working population in industrially developed countries.<sup>1</sup> Because the number of patients with DR and vision-threatening DR is expected to increase,<sup>2</sup> further research is warranted on the methods for evaluating clinical conditions of DR and on treatment advances.

Fluorescein angiography (FA) is a vitally important diagnostic tool for evaluating clinical fundus features of DR.<sup>3</sup> FA can detect primary vascular lesions (eg, microaneurysms) and advanced vascular abnormalities such as venous beading and intraretinal microvascular abnormalities (IRMA). Retinal nonperfusion, which represents intraretinal capillary occlusion or dropout, can be visualized as a dark area surrounded by large retinal vessels. Neovascularization can be identified by remarkable leakage of the dye toward the vitreous cavity. Diagnosis of DR progression using FA could be integral to enabling decisions on treatment indications; however, intravenous dye injections should be performed carefully because patients with severe DR tend to have systemic vascular complications such as severe renal disorder and clinical or subclinical cardiovascular disease.<sup>4–6</sup> Even in healthy subjects, dye injections can also occasionally cause nausea and, rarely but critically, anaphylaxis.<sup>7</sup> Furthermore, FA cannot separately visualize the intraretinal structures of the major capillary networks; the images of the superficial capillaries and deep capillaries overlap because FA images are limited to 2 dimensions.

Optical coherence tomography (OCT) is a noninvasive technique that provides micrometer-level axial resolution in cross-sectional retinal imaging and has been clinically adopted as the standard to observe structural changes of diabetic retinopathy, such as diabetic macular edema.<sup>8</sup> Recently, several theoretically based OCT angiography methods were developed for 3-dimensional noninvasive vascular mapping at the microcirculation level.<sup>9–18</sup> In particular, the use of the split-spectrum amplitude-decorrelation angiography algorithm improves the signal-to-noise ratio of flow detection;<sup>11</sup> thus, OCT angiography applying this algorithm can clearly visualize chorioretinal vascular lesions.<sup>13,14,16</sup> In this study, using newly developed OCT angiography, we evaluated its ability to visualize the pathologic vascular changes of DR, focusing especially on microaneurysms, retinal nonperfusion, and neovascularization.

Accepted for publication Apr 14, 2015.

From the Department of Ophthalmology, Asahikawa Medical University, Asahikawa, Japan.

Inquiries to Akihiro Ishibazawa, Department of Ophthalmology, Asahikawa Medical University, Midorigaoka Higashi 2-1-1-1, Asahikawa 078-8510, Japan; e-mail: [bazawa14@asahikawa-med.ac.jp](mailto:bazawa14@asahikawa-med.ac.jp)

## METHODS

• **STUDY POPULATION:** This prospective study evaluating imaging technology was conducted at Asahikawa Medical University from August 27, 2014, through November 24, 2014. The study was performed in adherence with the tenets of the Declaration of Helsinki and was approved prospectively by our institutional review board at the Asahikawa Medical University. Informed consent was obtained from all subjects to participate in this research. Twenty-five patients with diabetes mellitus were recruited. Patients diagnosed with DR underwent comprehensive ophthalmologic examinations, including measurement of the best-corrected visual acuity (BCVA), slit-lamp biomicroscopy, color fundus photography, FA, and OCT. The FA was performed with Spectralis HRA + OCT (Heidelberg Engineering, Heidelberg, Germany). Exclusion criteria were the presence of severe media opacities, such as severe cataract or vitreous hemorrhage.

• **OPTICAL COHERENCE TOMOGRAPHY ANGIOGRAPHY:** The instrument used for the OCT images was based on the RTVue XR Avanti (Optovue Inc, Fremont, California, USA) and was used to obtain OCT angiograms as previously described by Spaide and associates.<sup>15,16</sup> This instrument has an A-scan rate of 70 000 scans per second, using a light source centered on 840 nm and a bandwidth of 50 nm. The tissue resolution is 5  $\mu\text{m}$  axially and there is a 15- $\mu\text{m}$  beam width. Each B-scan contained 316 A-scans. Two consecutive B-scans (M-B frames) were captured at a fixed position before proceeding to the next sampling location. The volumes were registered and the B-scan images were compared to calculate the decorrelation in the images; the decorrelation was viewed as the maximal projection image of blood flow. Because the retina is a laminar structure with a corresponding stratification of blood supply, segmentation of the retina in specific layers allows simple en face visualization of the corresponding vascular supply in that layer.

The scanning area was captured in  $3 \times 3$ -mm sections and was centered on the fovea, on the optic disc head, or on the region of interest within 6 mm of the fovea or optic disc. We segmented OCT angiograms as follows. The ganglion cell layer is invested with 1 or more layers of capillaries.<sup>19,20</sup> The en face image was segmented with an inner boundary at 3  $\mu\text{m}$  beneath the internal limiting membrane and the outer boundary was set at 15  $\mu\text{m}$  beneath the inner plexiform layer (IPL) to obtain images of the superficial vascular layers (defined as superficial plexus). On the other hand, the inner nuclear layer is ordinarily bracketed by a layer of capillaries on either side.<sup>19,20</sup> The en face image was segmented with an inner boundary at 15  $\mu\text{m}$  beneath the IPL and the outer boundary was set at 70  $\mu\text{m}$  beneath the IPL to obtain

images of the deep vascular layers (defined as deep plexus). Regarding OCT angiograms around the optic disc head, the superficial vascular layers were imaged starting with the outer border of the vitreous cavity as reference and selecting sufficient thickness to include the ganglion cell layer. Figure 1 shows the OCT angiograms of superficial and deep plexuses centered on the fovea and a superficial OCT angiogram centered on the optic disc in a normal control case (62-year-old man). It also shows the layer segmentation in OCT B-scan for each OCT angiogram.

• **EVALUATION OF VASCULAR LESIONS AND STATISTICAL ANALYSIS:** For evaluation of microaneurysms in this pilot study, we used  $3 \times 3$ -mm images centered on the fovea. The criterion for classifying a lesion as a microaneurysm was a distinctly round hyperfluorescent spot in early- and/or late-phase FA.<sup>21,22</sup> Saccular capillary ends were considered to represent microaneurysms.<sup>21</sup> We investigated how the microaneurysms detected by FA could be depicted in the OCT angiograms. With regard to quantitative measurement of the retinal nonperfused area, we traced the border between the area in which no or few abnormal capillaries (representing capillary pruning<sup>23</sup>) were observed and the area in which dense capillaries were visualized within  $3 \times 3$ -mm sectional OCT angiograms of superficial and deep plexuses near the macula. We measured the traced area (expressed in  $\text{mm}^2$ ) using ImageJ 1.48 software (NIH, Bethesda, Maryland, USA). To quantify the vascular structural changes of neovascularization at the disc (NVD), the NVD flow area was calculated from the superficial OCT angiograms around the optic disc head. The NVD flow area of the same lesion above the disc was calculated by multiplying the number of pixels (for which the decorrelation value was above that of the background) and the pixel size<sup>13</sup> using the contained software (ReVue, version 2014.2.0.65; Optovue Inc, Fremont, California, USA).

Measurements of nonperfused area and NVD flow area represented the average data made by 2 observers (K.S. and T.T.) who were masked to the clinical status. The measured nonperfused areas on OCT angiograms were expressed as the mean  $\pm$  standard error of the mean. The Wilcoxon signed rank test was used to compare superficial nonperfused areas to the deep ones. SPSS statistics software version 19.0 (SPSS Inc, an IBM Company, Chicago, Illinois) was used for statistical analysis. A probability (*P*) value  $< .05$  was considered statistically significant.

## RESULTS

A TOTAL OF 47 EYES OF 25 PATIENTS (17 MALE AND 8 FEMALE) with DR at different stages were imaged using the RTVue

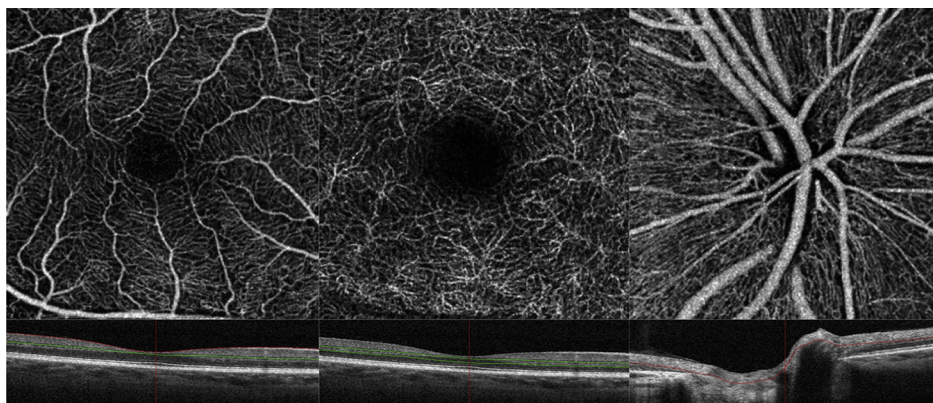


**FIGURE 1.** En face optical coherence tomography (OCT) angiography images (Top row) and horizontal B-scan images of their layer segmentation (Bottom row) in a healthy control individual (62-year-old man). (Top left) OCT angiogram of a superficial vascular plexus in a  $3 \times 3$ -mm area centered on the macula. (Bottom left) The en face image of the superficial plexus was segmented with an inner boundary at  $3 \mu\text{m}$  beneath the internal limiting membrane and the outer boundary was set at  $15 \mu\text{m}$  beneath the inner plexiform layer. (Top center) The OCT angiogram of a deep capillary plexus in a  $3 \times 3$ -mm area centered on the macula. (Bottom center) The image of the deep plexus was segmented with an inner boundary at  $15 \mu\text{m}$  beneath the inner plexiform layer, and the outer boundary was set at  $70 \mu\text{m}$  beneath the inner plexiform layer. (Top right) An OCT angiogram of a superficial vascular layer in a  $3 \times 3$ -mm area centered on the optic disc. (Bottom right) The OCT angiogram of the disc was imaged starting with the outer border of the vitreous cavity as a reference and selecting sufficient thickness to include the ganglion cell layer.

XR Avanti and OCT angiograms around the macula and optic disc were obtained. The patients ranged in age from 32 to 78 years, with a mean age of 61 years. According to the International Clinical Diabetic Retinopathy and Diabetic Macula Edema Disease Severity Scales,<sup>24</sup> there were 11 eyes with mild nonproliferative diabetic retinopathy (NPDR), 13 eyes with moderate NPDR, 12 eyes with severe NPDR, and 11 eyes with proliferative diabetic retinopathy (PDR) in this study. Three eyes were excluded because they could not be scanned with OCT angiography owing to severe cataract (2 eyes) and vitreous hemorrhage (1 eye).

• **MICROANEURYSMS EVALUATED WITH FLUORESCEIN ANGIOGRAPHY AND OPTICAL COHERENCE TOMOGRAPHY ANGIOGRAPHY:** Scattered microaneurysms were detected as hyperfluorescent dots in the early and/or late phases of FA images. In 42 eyes, most of the microaneurysms were identified as focally dilated saccular or fusiform capillaries in the  $3 \times 3$ -mm area of the en face OCT angiograms centered on the fovea. The OCT angiographic technique could visualize the origin of microaneurysms within the layers: microaneurysms originated from the superficial and/or deep plexus. A typical case in which microaneurysms were visualized by OCT angiograms is shown in Figure 2. This was a 70-year-old woman who had moderate NPDR with slight macular edema in her left eye with a BCVA of 20/25. FA showed many hyperfluorescent spots representing microaneurysms in the early and/or late phase. On OCT angiograms, microaneurysms were visualized as demarcated saccular or fusiform shapes of focally dilated capillary vessels in the superficial and deep plexuses (Figure 2). Besides this, some hyperfluorescent spots on FA images were not clearly

visualized on any OCT angiograms of the superficial or deep plexus. Conversely, some well-demarcated and dot-like capillaries on OCT angiograms closely resembled other microaneurysms in appearance but were not depicted by FA. No MAs were observed on OCT angiograms of the outer retina (data not shown).

• **VISUALIZATION AND QUANTIFICATION OF RETINAL NONPERFUSED AREAS:** Areas of retinal nonperfusion were visualized by FA as a dark area between the relatively large retinal vessels, which represented intraretinal capillary occlusion or dropout. The edge of the retinal nonperfused area near the optic disc and the macula could be observed by OCT angiography as an area where capillaries could not be observed. Residual, irregular capillaries were also clearly observed in the edges of nonperfused areas by OCT angiography. Typical examples are shown in Figures 3 (near the optic disc) and 4 (near the macula). A 60-year-old man noticed decreased visual acuity for several years in both eyes. BCVA in his left eye was 20/25. The eye was characterized by mild cataract and severe NPDR (Figure 3). FA showed extensive nonperfused areas in the nasal retina and venous beading at the superior nasal venule. On an OCT angiogram of the superficial vascular layer near the optic disc, retinal nonperfused areas were clearly visualized as a capillary-nonvisible area (Figure 3). Intraretinal irregular capillaries, faintly visualized by FA in the edge of nonperfused areas between the superior large vessels near the optic disc, were clearly observed as dilated, looped, and coarse capillaries by OCT angiography. Furthermore, OCT angiography enabled the visualization of their branching points to



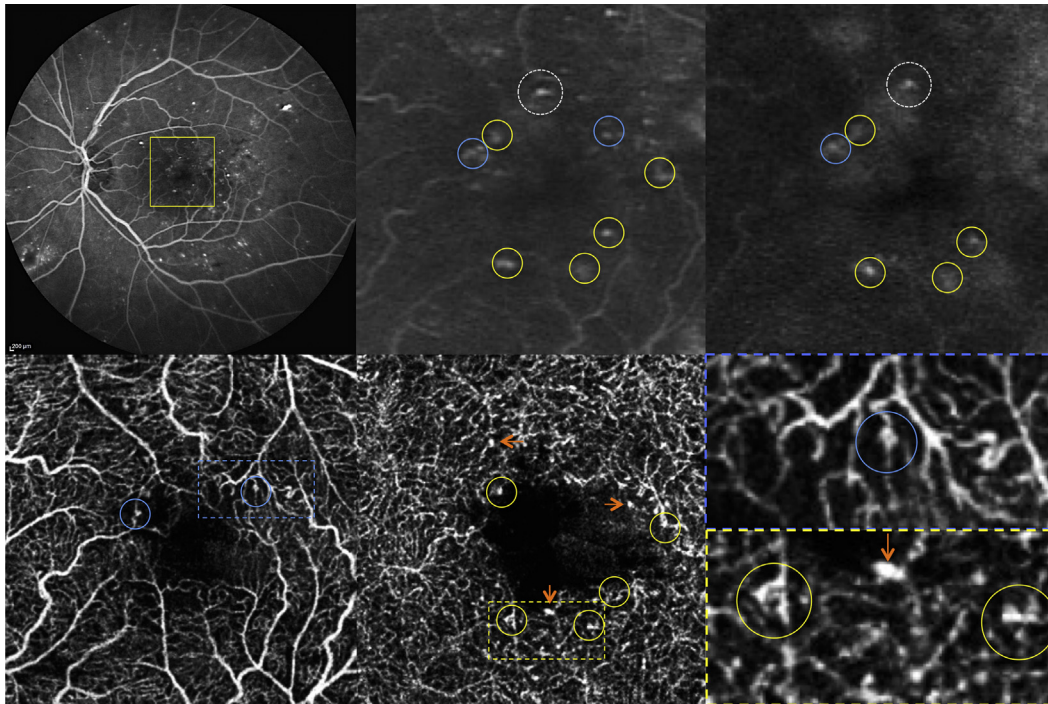


**FIGURE 2.** Optical coherence tomography (OCT) angiography showing multiple microaneurysms in a case of moderate nonproliferative diabetic retinopathy (70-year-old woman). (Top left) Early-phase fluorescein angiography (FA). The yellow square outlines the area shown on the angiograms below. (Top center) Magnified view of early-phase FA is shown within the yellow square. Blue and yellow circles indicate multiple microaneurysms. A white-dot circle also indicates a microaneurysm, which was not depicted by OCT angiography. (Top right) Magnified view of late-phase FA. (Bottom left) OCT angiogram of the superficial vascular plexus. Blue circles indicate saccular shapes of dilated capillary vessels (ie, microaneurysms) matching those in the FA images. (Bottom center) An OCT angiogram of the deep capillary plexus. Yellow circles indicate saccular and fusiform shapes of dilated capillary vessels (ie, microaneurysms) matching those in the FA images. Orange arrows indicate microaneurysm-like forms of capillaries seen in the OCT angiograms, but not visualized by FA. (Bottom right) Magnified view of the blue and yellow rectangle in the OCT angiograms of the superficial and deep plexus, respectively.

superficial, large retinal venules. In another case, a 50-year-old woman diagnosed with type 2 diabetes mellitus about 15 years prior to the study had dropped out early from therapy. BCVA of both eyes was 20/20, but FA examination revealed extensive retinal nonperfusion and substantial neovascularization; therefore, the patient was diagnosed with PDR (Figure 4). Focusing on the area near the macula, an edge of the large nonperfused area of the temporal retina was observed. On OCT angiograms of the same region as that in the FA image, the nonperfused areas in the superficial and deep plexuses were traced as dotted lines, and several intraretinal abnormal capillaries (residual coarse capillaries) were also observed at the edge of nonperfused areas (Figure 4). The traced nonperfused areas in the superficial and deep plexuses on OCT angiograms were measured to be  $3.66 \text{ mm}^2$  and  $3.07 \text{ mm}^2$ , respectively. We also quantitatively analyzed the nonperfused areas around the macula in 7 eyes on OCT angiograms. The retinal nonperfused areas in the superficial plexus ( $3.67 \pm 0.69 \text{ mm}^2$ ) were significantly larger than those in the deep plexus ( $3.02 \pm 0.59 \text{ mm}^2$ ,  $P = .018$ ).

• **VISUALIZATION OF VASCULAR STRUCTURES OF NEOVASCULARIZATION AND QUANTITATIVE EVALUATION:** In the 4 eyes with PDR, vascular structures of the NVD could be visualized clearly on OCT angiograms. In 1 case, the changes of NVD after anti-vascular endothelial growth factor (VEGF) therapy were quantitatively observed (Figures 5 and 6). A 32-year-old man was diagnosed with PDR in both eyes 6 months prior to study and immediately received panretinal photocoagulation. The condition of PDR, however, progressively worsened and the patient developed neovascular glaucoma and severe macular edema. Fundus photography and FA demonstrated a marked, fibrovascular membrane including NVD, but the vascular structures of NVD could not be visualized because of excessive leakage from NV even in the early phase of FA (Figure 5). However, the OCT angiogram of the optic disc clearly showed massive neovascular structures in the fibrovascular membrane above the optic disc (Figure 5). Two weeks after intravitreal injection of an anti-VEGF agent (ranibizumab), NVD was remarkably reduced and iris rubeosis and macular edema disappeared. The NVD area

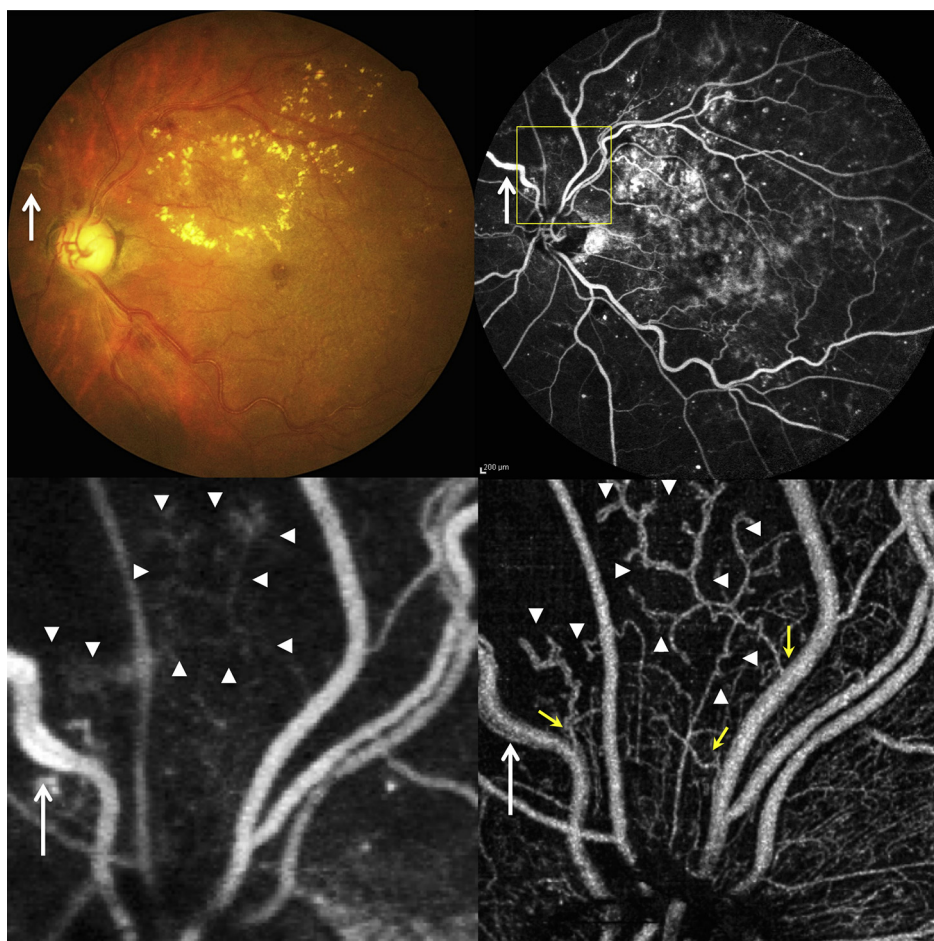


**FIGURE 3.** Optical coherence tomography (OCT) angiography showing retinal nonperfusion near the optic disc in a case of severe nonproliferative diabetic retinopathy (60-year-old man). (Top left) Color fundus photograph. The white arrow indicates venous beading in the superior nasal venule. (Top right) Early-phase fluorescein angiography (FA) shows extensive areas of retinal nonperfusion in the nasal retina. The white arrow indicates venous beading with hyperfluorescence of the venous wall. (Bottom left) Magnified view of early-phase FA within the yellow square. White arrowheads indicate intraretinal irregular capillaries in the edge of the nonperfused area between the superior large vessels near the optic disc. (Bottom right) An OCT angiogram of the superficial vascular layer near the optic disc. The nonperfused area is seen as a capillary-nonvisible area. White arrowheads indicate irregular capillaries, matching those seen in the FA image. Yellow arrows indicate their branching points to superficial large retinal venules.

had further decreased 4 weeks after the injection, although spiral, looped, and irregular microvasculature in the optic disc remained. However, 8 weeks after the injection, the diameter of the abnormal vessels comprising NVD was enlarged and the amount of irregular vasculature had increased; thus, NVD had regrown and was revitalized (Figure 5). The changes in the NVD flow area were quantitatively evaluated (Figure 6). The NVD flow area had decreased as time had passed, but was still increased 8 weeks after the injection of ranibizumab.

## DISCUSSION

RECENT OCT ANGIOGRAPHIC STUDIES USING THE new split-spectrum amplitude-decorrelation angiography

algorithm presented detailed images of choroidal neovascularization<sup>13</sup>; dense and decreased microvascular networks in normal and glaucomatous optic discs, respectively<sup>14</sup>; and the alternation of the inner/outer retinal vascular plexus and invasion into the outer and subretinal space in the eyes with macular telangiectasia type 2.<sup>16</sup> The current study demonstrated that en face OCT angiograms could clearly visualize the different vascular lesions in different stages of DR. Microaneurysms were identified as focally dilated and abnormally shaped capillaries, the location of which could be evaluated in the superficial and deep vascular plexuses. The extent of retinal nonperfusion, visualized as no-flow or sparse-capillary areas, could also be evaluated differently in each layer. Moreover, the dynamic change in the abnormal vasculature in NVD could be readily observed and quantified.



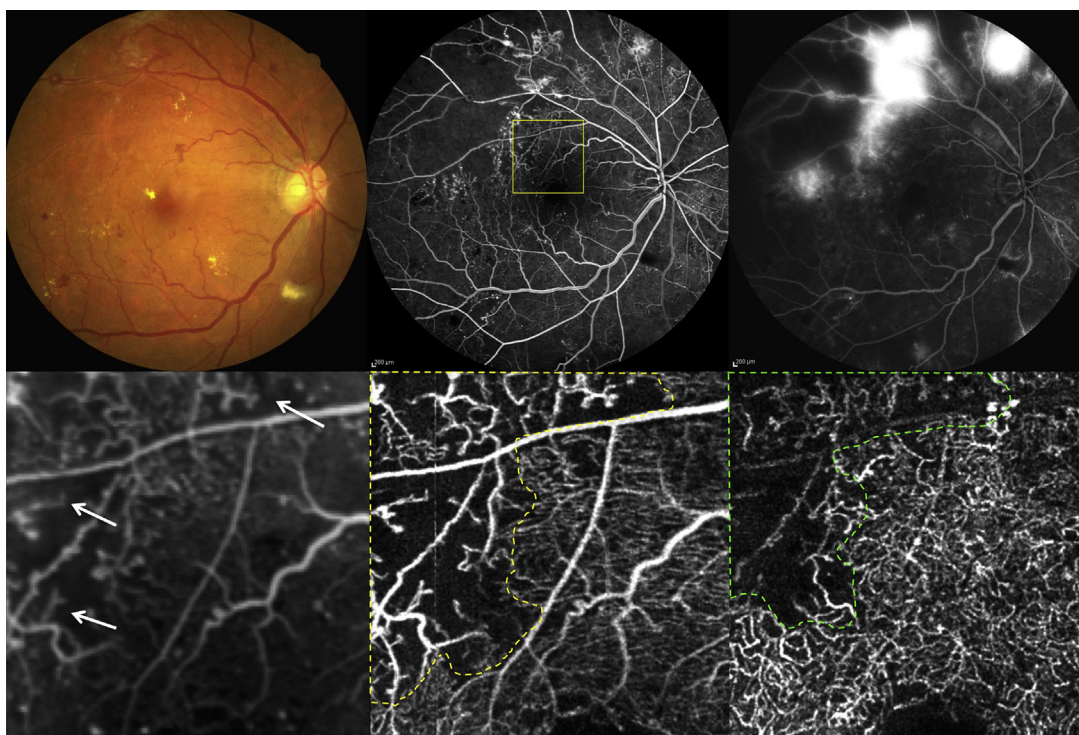


**FIGURE 4.** Optical coherence tomography (OCT) angiography showing retinal nonperfusion near the macula in a case of proliferative diabetic retinopathy (50-year-old woman). (Top left) Color fundus photograph. (Top center) Early-phase fluorescein angiography (FA) showing widespread retinal nonperfusion in the temporal retina and substantial neovascularization elsewhere. The yellow square outlines the area shown in the angiograms below. (Top right) Late-phase FA. (Bottom left) Magnified view of early-phase FA is seen within the yellow square. White arrows indicate the edge of a large nonperfused area in the temporal retina. (Bottom center) The OCT angiogram of the superficial vascular plexus. A yellow dotted line indicates the border between the area with no or few abnormal capillaries and the area with dense capillaries (ie, the nonperfused area) in the superficial plexus. (Bottom right) An OCT angiogram of the deep capillary plexus. A green dotted line indicates the nonperfused area in the deep plexus.

Microaneurysms, which are observed as hyperfluorescent spots in early and/or late phase in FA, are the first clinically detectable sign of early DR.<sup>22</sup> Previous histopathologic studies demonstrated that microaneurysms were defined as any focal capillary dilation, and the morphology of microaneurysms was characterized by saccular, fusiform, and focal bulges.<sup>25,26</sup> On OCT angiograms, the microaneurysms observed in FA were seen as focally dilated saccular or fusiform capillaries (Figure 2), which appeared to be similar morphologically to microaneurysms observed microscopically.<sup>25,26</sup> Regarding the location of microaneurysms, the majority of these (around 80%) were seen to be located in the inner nuclear layer and its inner/outer borders (ie, deep plexus) in a histologic study<sup>26</sup> and in a clinicopathologic study using OCT.<sup>27</sup> The OCT angiography in the current study also showed that the microaneurysms were located mainly in the deep plexus. Although we defined microaneurysms as hyperfluorescent spots in the early and/or late phases of FA,<sup>21,22</sup> there was incomplete agreement between MAs shown on FA and those on OCT angiograms, as Schwartz and associates recently described using phase-variance

OCT.<sup>12</sup> Histopathologic studies have reported that the lumen configuration in microaneurysms consists of diverse components such as thickened, hyalinized, fibrous, laminated, and lipid-containing basement membrane, as well as hypercellular or multilayered endothelial cells.<sup>25</sup> Therefore, the blood flow inside microaneurysms could be turbulent. These results suggest that the blood flow inside some types of microaneurysms may not have been perfectly displayed using OCT angiography. Furthermore, hyperfluorescent dots observed on FA may not always represent microaneurysms but instead may represent focal leakage from impaired retinal capillaries. Conversely, the pinpoint spots observed by OCT angiography and not by FA may simply be capillary ends or vertically oriented capillaries (Figure 2). Higher-resolution imaging in OCT angiography is needed to assess the specificity of microaneurysm detection.

Angiographically hypofluorescent areas representing capillary occlusion or capillary pruning/dropout are regarded as areas of retinal ischemia,<sup>23</sup> that is, retinal nonperfusion. The edge of nonperfused areas was fuzzy in FA; however, OCT angiograms clearly visualized the

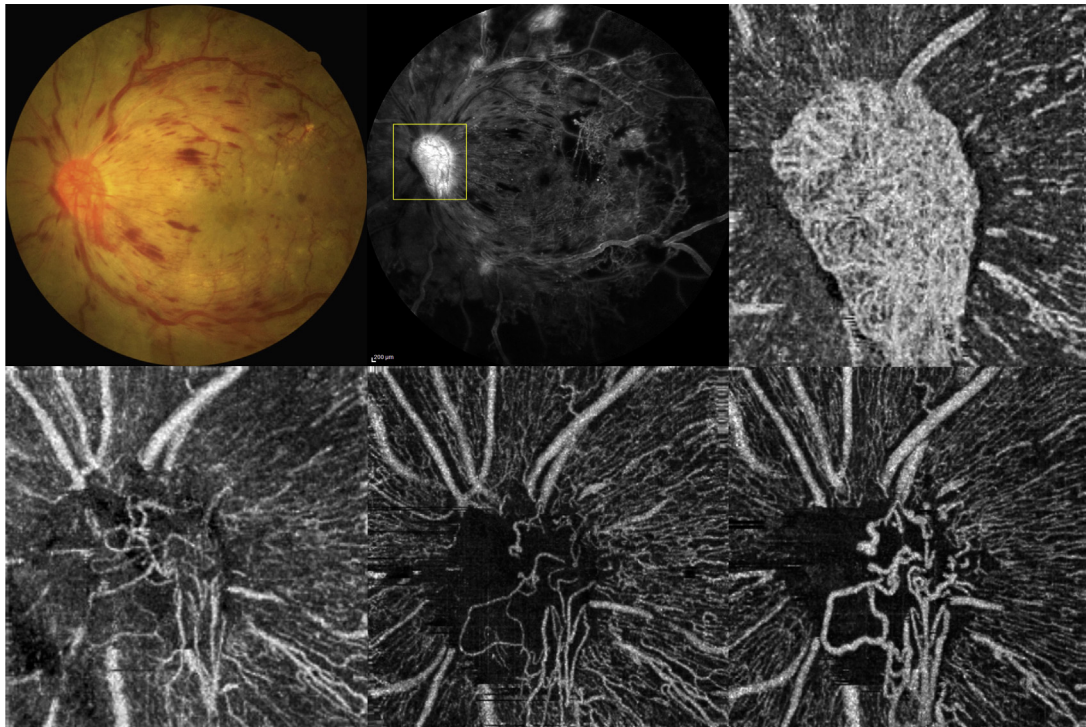


**FIGURE 5.** Optical coherence tomography (OCT) angiography showing neovascularization at the disc (NVD) in a case of proliferative diabetic retinopathy (32-year-old man). (Top left) Color fundus photograph showing a fibrovascular membrane including NVD. (Top center) Early-phase fluorescein angiography showing excessive leakage from NVD. The detailed vascular structures of NVD could not be visualized. The yellow square outlines the area shown in the angiograms below. (Top right) An OCT angiogram of the optic disc. Massive structures of neovascularization in the fibrovascular membrane above the optic disc are clearly seen. (Bottom left) An OCT angiogram taken 2 weeks after intravitreal injection of ranibizumab. Neovascular vessels are remarkably reduced. (Bottom center) An OCT angiogram taken 4 weeks after ranibizumab injection. The NVD area has further decreased. Spiral, looped, and irregular microvasculature remains on the optic disc. (Bottom right) An OCT angiogram taken 8 weeks after the ranibizumab injection. The diameter of the abnormal vessels composing NVD has enlarged, and an increase in irregular vasculature can be observed.

border between sparse-capillary areas and dense-capillary areas (Figures 3 and 4). We measured the nonperfused area and demonstrated that the average area of retinal nonperfusion in the superficial plexus was slightly larger than that in the deep plexus (Figure 4). To our knowledge, there is no histopathologic evidence of the difference between the extent of retinal nonperfusion in superficial and deep plexuses. Microvascular networks in the deep plexus near the macula have been reported to be well developed in the inner and outer border of the inner nuclear layer<sup>19,20</sup>; therefore, these results might suggest that deep capillaries could to a certain extent be spared from microthrombosis compared with superficial ones. A larger study is required to study this phenomenon in detail. At the edges of nonperfused areas, a few dilated, looped, coarse, and irregular capillaries were visualized, especially on superficial OCT angiograms (Figures 3 and 4). Because the thickness of the inner retina in the nonperfused area was thinner than that of normal parts of the retina as previously described,<sup>28</sup> these superficial, dilated, irregular capillaries were also visualized in the

deeper images, apparently anastomosing with the truncated and the deeper capillaries (Figures 3 and 4). These irregular capillaries were estimated to represent residual microvasculature (resulting in capillary occlusion/dropout), developing as tortuous, abnormal shunts (ie, the clinical term IRMA),<sup>29</sup> or intraretinal neovascularization.<sup>30</sup>

Neovascularization toward the vitreous cavity with remarkable leakage visualized by FA is the diagnostic hallmark of PDR. Suzuma and associates demonstrated that a scanning laser confocal ophthalmoscope could visualize neovascular vessels in fibrovascular membranes before and after anti-VEGF therapy.<sup>31</sup> However, the images could not directly visualize the new vessels containing blood-flow information. Most recently, Miura and associates<sup>18</sup> reported that Doppler OCT images provided the 3-dimensional extent of new vessels at various stages of neovascularization with blood-flow information in eyes with PDR because the Doppler imaging was impervious to leakage from new vessels. On the other hand, OCT angiography, which is also unaffected by fluorescein leakage

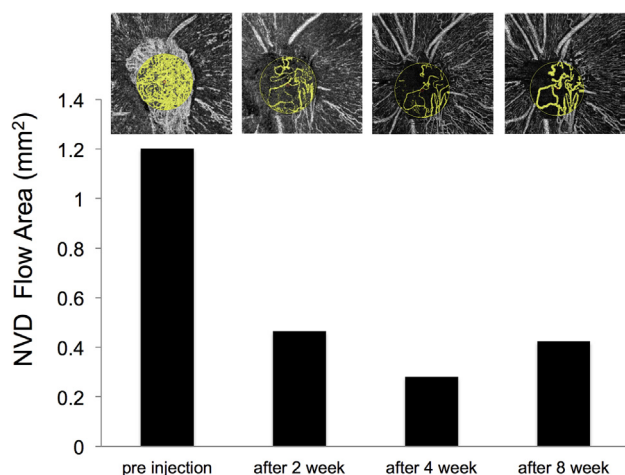


**FIGURE 6.** Quantitative evaluation in neovascularization at the disc (NVD) flow area in OCT angiograms (Figure 5) before and after intravitreal injection of ranibizumab. The NVD flow area at the same lesion decreased as time passed but re-increased 8 weeks after the ranibizumab injection.

and visualizes the blood flow inside the vessels, could clearly describe the abnormal NVD vascular structures (Figure 5). We also quantitatively showed, for the first time, the course of decrease and re-increase of blood flow in new vessels after anti-VEGF therapy (Figure 6). A previous histologic study showed that apoptotic vascular endothelial cells in proliferative tissue and no apparent fenestration in newly formed vessels could be observed after intravitreal injection of bevacizumab.<sup>32</sup> Furthermore, Suzuma and associates<sup>31</sup> showed that the many neovascular capillaries were still present in neovascular tissue after the bevacizumab treatment but only large vessels contained red blood cells. Kubota and associates<sup>33</sup> demonstrated that vascular endothelial cells with decreased expression of VEGF were still present in the proliferative tissues after the bevacizumab injection. Our data may support the suggestion made by Kubota and associates that anti-VEGF therapy temporally reduces the blood flow of the new vessels; however, it did not induce complete regression of the vascular endothelial cells in new vessels.<sup>33</sup> Therefore, the blood flow of new vessels may be easily reperfused when the effect of anti-VEGF therapy has diminished.

The current study had some limitations. First, we tried numerous evaluations of microaneurysms identified by FA and OCT angiography, but we encountered the above-mentioned difficulties in terms of specificity in

microaneurysm detection. Unless histopathologic methods could be used, we cannot definitively confirm that the pinpoint spots observed with FA and OCT angiography were true microaneurysms. Recent studies have demonstrated that a high microaneurysm formation rate can be a predictive marker for progression to clinically significant macular edema,<sup>34</sup> and ranibizumab treatment can affect microaneurysm turnover with NPDR using an automated computer-aided system capable of detecting microaneurysms.<sup>35</sup> Because OCT angiography can noninvasively and repeatedly scan the same lesions, temporal microaneurysm turnover in the same capillaries might be evaluated to assess the activity of DR even if all microaneurysms cannot be visualized by OCT angiography. The second limitation was that OCT angiograms obtained by the RTVue OCT provided only a 3-mm-square field of view if we required sufficient quality of images that could clearly visualize the capillary network. We observed the edge of retinal nonperfused areas and quantified these areas near the macula on the small OCT angiograms; however, the nonperfused area extended to the peripheral retina. To evaluate the difference between intraretinal vascular abnormalities in the superficial plexus and those in the deep plexus in the peripheral nonperfused area, a larger field of view on OCT angiograms will be required. A third limitation was that the changes in vessels visualized on OCT angiograms did not directly indicate the structural regression and regeneration of neovascular vessels and capillary dropout, because the OCT angiograms depicted blood flow only. Therefore, the decrease in blood flow in neovascular vessels may indicate decreased activity of neovascular vessels but may not always demonstrate the disappearance of neovascular structures. As well as the retinal nonperfused area, capillary occlusion and capillary dropout (ie, complete loss of capillaries) cannot be differentiated. A fourth limitation was that OCT angiography could not evaluate the breakdown of the blood-retinal barrier, which was represented by fluorescein leakage in FA. Hyperpermeability in the retinal vascular lesions is an important indication of retinal edema and neovascularization; therefore FA is, of course, an essential diagnostic modality for DR.

In conclusion, this pilot study demonstrates that OCT angiography can clearly visualize microaneurysms and retinal nonperfusion, enabling a closer observation of each layer of the retinal capillaries. Quantitative information in neovascular vessels can also be obtained. OCT angiography may be clinically useful to evaluate the microvascular status and therapeutic effect of treatments for DR.

ALL AUTHORS HAVE COMPLETED AND SUBMITTED THE ICMJE FORM FOR DISCLOSURE OF POTENTIAL CONFLICTS OF INTEREST. Financial Disclosures: Akihiro Ishibazawa received lecture fees from Novartis Pharma AG (Basel, Switzerland), and Chuo Sangio Co (Nishimiya, Japan). The other authors have no proprietary/financial interest. Funding/Support: This study was supported by a Grant-in-Aid for Young Scientists (B) 25861608 (A.I.) and Scientific Research (B) 25293352 (T.N.) from the Japan Society for the Promotion of Science, Tokyo, Japan. All authors attest that they meet the current ICMJE requirements to qualify as authors.

The authors thank Tomoko Mase (Asahikawa Medical University, Asahikawa, Japan) for contribution to data collection.



## REFERENCES

1. Klein R, Klein BE, Moss SE, Davis MD, DeMets DL. The Wisconsin epidemiologic study of diabetic retinopathy. III. Prevalence and risk of diabetic retinopathy when age at diagnosis is 30 or more years. *Arch Ophthalmol* 1984;102(4):527–532.
2. Saaddine JB, Honeycutt AA, Narayan KM, Zhang X, Klein R, Boyle JP. Projection of diabetic retinopathy and other major eye diseases among people with diabetes mellitus: United States, 2005–2050. *Arch Ophthalmol* 2008;126(12):1740–1747.
3. Gass JD. A fluorescein angiographic study of macular dysfunction secondary to retinal vascular disease. IV. Diabetic retinal angiopathy. *Arch Ophthalmol* 1968;80(5):583–591.
4. Cheung N, Wang JJ, Klein R, Couper DJ, Sharrett AR, Wong TY. Diabetic retinopathy and the risk of coronary heart disease: the Atherosclerosis Risk in Communities Study. *Diabetes Care* 2007;30(7):1742–1746.
5. Kawasaki R, Cheung N, Islam FM, et al. Is diabetic retinopathy related to subclinical cardiovascular disease? *Ophthalmology* 2011;118(5):860–865.
6. Fioretto P, Mauer M, Brocco E, et al. Patterns of renal injury in NIDDM patients with microalbuminuria. *Diabetologia* 1996;39(12):1569–1576.
7. Kwiterovich KA, Maguire MG, Murphy RP, et al. Frequency of adverse systemic reactions after fluorescein angiography. Results of a prospective study. *Ophthalmology* 1991;98(7):1139–1142.
8. Yeung L, Lima VC, Garcia P, Landa G, Rosen RB. Correlation between spectral domain optical coherence tomography findings and fluorescein angiography patterns in diabetic macular edema. *Ophthalmology* 2009;116(6):1158–1167.
9. Mariampillai A, Standish BA, Moriyama EH, et al. Speckle variance detection of microvasculature using swept-source optical coherence tomography. *Opt Lett* 2008;33(13):1530–1532.
10. Miura M, Makita S, Iwasaki T, Yasuno Y. Three-dimensional visualization of ocular vascular pathology by optical coherence angiography in vivo. *Invest Ophthalmol Vis Sci* 2011;52(5):2689–2695.
11. Jia Y, Tan O, Tokayer J, et al. Split-spectrum amplitude-decorrelation angiography with optical coherence tomography. *Opt Express* 2012;20(4):4710–4725.
12. Schwartz DM, Fingler J, Kim DY, et al. Phase-variance optical coherence tomography: a technique for noninvasive angiography. *Ophthalmology* 2014;121(1):180–187.
13. Jia Y, Bailey ST, Wilson DJ, et al. Quantitative optical coherence tomography angiography of choroidal neovascularization in age-related macular degeneration. *Ophthalmology* 2014;121(7):1435–1444.
14. Jia Y, Wei E, Wang X, et al. Optical coherence tomography angiography of optic disc perfusion in glaucoma. *Ophthalmology* 2014;121(7):1322–1332.
15. Spaide RF, Klancnik JM Jr, Cooney MJ. Retinal vascular layers imaged by fluorescein angiography and optical coherence tomography angiography. *JAMA Ophthalmol* 2015;133(1):45–50.
16. Spaide RF, Klancnik JM Jr, Cooney MJ. Retinal vascular layers in macular telangiectasia type 2 imaged by optical coherence tomographic angiography. *JAMA Ophthalmol* 2015;133(1):66–73.
17. Huang Y, Zhang Q, Thorell MR, et al. Swept-source OCT angiography of the retinal vasculature using intensity differentiation-based optical microangiography algorithms. *Ophthalmic Surg Lasers Imaging Retina* 2014;45(5):382–389.
18. Miura M, Hong YJ, Yasuno Y, Muramatsu D, Iwasaki T, Goto H. Three-dimensional vascular imaging of proliferative diabetic retinopathy by Doppler optical coherence tomography. *Am J Ophthalmol* 2015;159(3):528–538.
19. Snodderly DM, Weinhaus RS, Choi JC. Neural-vascular relationships in central retina of macaque monkeys (*Macaca fascicularis*). *J Neurosci* 1992;12(4):1169–1193.
20. Weinhaus RS, Burke JM, Delori FC, Snodderly DM. Comparison of fluorescein angiography with microvascular anatomy of macaque retinas. *Exp Eye Res* 1995;61(1):1–16.
21. Hellstedt T, Immonen I. Disappearance and formation rates of microaneurysms in early diabetic retinopathy. *Br J Ophthalmol* 1996;80(2):135–139.
22. Jalli PY, Hellstedt TJ, Immonen IJ. Early versus late staining of microaneurysms in fluorescein angiography. *Retina* 1997;17(3):211–215.
23. Wessel MM, Nair N, Aaker GD, Ehrlich JR, D'Amico DJ, Kiss S. Peripheral retinal ischaemia, as evaluated by ultra-widefield fluorescein angiography, is associated with diabetic macular oedema. *Br J Ophthalmol* 2012;96(5):694–698.
24. Wilkinson CP, Ferris FL 3rd, Klein RE, et al. Proposed international clinical diabetic retinopathy and diabetic macular edema disease severity scales. *Ophthalmology* 2003;110(9):1677–1682.
25. Stitt AW, Gardiner TA, Archer DB. Histological and ultrastructural investigation of retinal microaneurysm development in diabetic patients. *Br J Ophthalmol* 1995;79(4):362–367.
26. Moore J, Bagley S, Ireland G, McLeod D, Boulton ME. Three dimensional analysis of microaneurysms in the human diabetic retina. *J Anat* 1999;194(Pt 1):89–100.
27. Horii T, Murakami T, Nishijima K, Sakamoto A, Ota M, Yoshimura N. Optical coherence tomographic characteristics of microaneurysms in diabetic retinopathy. *Am J Ophthalmol* 2010;150(6):840–848.
28. Unoki N, Nishijima K, Sakamoto A, et al. Retinal sensitivity loss and structural disturbance in areas of capillary nonperfusion of eyes with diabetic retinopathy. *Am J Ophthalmol* 2007;144(5):755–760.
29. Grading diabetic retinopathy from stereoscopic color fundus photographs—an extension of the modified Airlie House classification. ETDRS report number 10. Early Treatment Diabetic Retinopathy Study Research Group. *Ophthalmology* 1991;98(5 Suppl):786–806.
30. Muraoka K, Shimizu K. Intraretinal neovascularization in diabetic retinopathy. *Ophthalmology* 1984;91(12):1440–1446.
31. Suzuma K, Tsuike E, Matsumoto M, Fujikawa A, Kitaoka T. Retro-mode imaging of fibrovascular membrane in proliferative diabetic retinopathy after intravitreal bevacizumab injection. *Clin Ophthalmol* 2011;5:897–900.
32. Kohno R, Hata Y, Mochizuki Y, et al. Histopathology of neovascular tissue from eyes with proliferative diabetic retinopathy after intravitreal bevacizumab injection. *Am J Ophthalmol* 2010;150(2):223–229.

33. Kubota T, Morita H, Tou N, et al. Histology of fibrovascular membranes of proliferative diabetic retinopathy after intravitreal injection of bevacizumab. *Retina* 2010;30(3):468–472.
34. Haritoglou C, Kernt M, Neubauer A, et al. Microaneurysm formation rate as a predictive marker for progression to clinically significant macular edema in nonproliferative diabetic retinopathy. *Retina* 2014;34(1):157–164.
35. Leicht SF, Kernt M, Neubauer A, et al. Microaneurysm turnover in diabetic retinopathy assessed by automated RetmarkerDR image analysis—potential role as biomarker of response to ranibizumab treatment. *Ophthalmologica* 2014;231(4):198–203.

## REPORTING VISUAL ACUITIES

The AJO encourages authors to report the visual acuity in the manuscript using the same nomenclature that was used in gathering the data provided they were recorded in one of the methods listed here. This table of equivalent visual acuities is provided to the readers as an aid to interpret visual acuity findings in familiar units.

Table of Equivalent Visual Acuity Measurements

Snellen Visual Acuities				
4 Meters	6 Meters	20 Feet	Decimal Fraction	LogMAR
4/40	6/60	20/200	0.10	+1.0
4/32	6/48	20/160	0.125	+0.9
4/25	6/38	20/125	0.16	+0.8
4/20	6/30	20/100	0.20	+0.7
4/16	6/24	20/80	0.25	+0.6
4/12.6	6/20	20/63	0.32	+0.5
4/10	6/15	20/50	0.40	+0.4
4/8	6/12	20/40	0.50	+0.3
4/6.3	6/10	20/32	0.63	+0.2
4/5	6/7.5	20/25	0.80	+0.1
4/4	6/6	20/20	1.00	0.0
4/3.2	6/5	20/16	1.25	−0.1
4/2.5	6/3.75	20/12.5	1.60	−0.2
4/2	6/3	20/10	2.00	−0.3

From Ferris FL III, Kassoff A, Bresnick GH, Bailey I. New visual acuity charts for clinical research. *Am J Ophthalmol* 1982;94:91–96.



### **Biosketch**

Akihiro Ishibazawa, MD, PhD, is a Clinical Fellow in the Department of Ophthalmology, Asahikawa Medical University, Asahikawa, Japan. He received his MD and PhD from Asahikawa Medical University. His clinical and research interests include diagnosis and treatment of chorioretinal disorders, ocular circulation, and retinal and choroidal imaging by optical coherence tomography.